



CHALMERS
UNIVERSITY OF TECHNOLOGY

Core–Shell Droplet Generation in an On-Chip Temperature Gradient

Downloaded from: <https://research.chalmers.se>, 2026-04-10 09:58 UTC

Citation for the original published paper (version of record):

Liu, R., Guarguati, C., Pelan, E. et al (2025). Core–Shell Droplet Generation in an On-Chip Temperature Gradient. *European Journal of Lipid Science and Technology*, 127(12).
<http://dx.doi.org/10.1002/ejlt.70066>

N.B. When citing this work, cite the original published paper.

RESEARCH ARTICLE OPEN ACCESS

Core–Shell Droplet Generation in an On-Chip Temperature Gradient

Rui Liu¹ | Carolina Gomez Guarguati² | Eddie Pelan² | Bettina Wolf² | Aldo Jesorka¹¹Department of Chemistry and Chemical Engineering, Chalmers University of Technology, Göteborg, Sweden | ²School of Chemical Engineering, University of Birmingham, Birmingham, UK**Correspondence:** Aldo Jesorka (aldo.jesorka@gomod.eu)**Received:** 25 January 2025 | **Revised:** 24 July 2025 | **Accepted:** 16 August 2025**Funding:** This study was supported by the European Union's Horizon 2020 research and innovation program under the Marie Skłodowska-Curie (Grant 956248).**Keywords:** core–shell droplets | microfluidics | poly(dimethyl siloxane) (PDMS) | semi-solid crystal | temperature gradient

ABSTRACT

We present a microfluidic device and associated heating/cooling setup for the generation of droplets stabilized by a lipid-crystalline shell. A conventional flow-focusing microfluidic droplet generator with 31 μm feature size was equipped with an on-chip resistive heater and placed on a microscope stage Peltier cooler in order to generate and isolate oil-in-water droplets enveloped by a crystalline shell of glycerol monostearate (GMS). A proof-of-concept protocol was developed for droplet generation over a temperature range between 60°C and 6°C, and GMS-coated droplets with a size between 13 and 49 μm were collected.

Practical application: Stabilized oil droplets of controlled size with a long shelf life and high thermal stability are of importance in various food applications. Improved emulsion stabilization prolongs retention of food quality. The GMS shell can efficiently preserve and protect sensitive cargo, such as flavors and nutrients. Reinforced droplets can also act as fat mimetics in low-fat or vegan formulations, help tailor mouthfeel, and enhance creaminess as well as spreadability. Given the size range of the particles produced, applications as microreactors for enzymatic reactions, which could enable new textures or flavors via micro-scale processing, are conceivable.

1 | Introduction

The aim of this study was to design a microfluidic device which would allow the study of the formation mechanism and the stability of lipid-crystalline shell-coated oil droplets. This droplet microstructure is commonly referred to as core–shell droplets, with applications ranging from the encapsulation of actives for targeted release upon breaking down the shell at the intended site of delivery to taste masking of hydrophobic bioactives in food applications [1]. We focused on generating, processing, and stabilizing emulsion droplets, enabled by the addition of a crystallizing surface-active lipid to the emulsion oil phase and the application of appropriate temperature profiles in the droplet break-up and

droplet stabilization phase. Lipid crystallization at interfaces in emulsified systems has been extensively reviewed by Douaire et al. [2] who provided details on mechanisms and key parameters as well as applications, among them droplet stabilization in Pickering emulsions and crystalline shells. For brevity, the core–shell droplets are termed particles in the following. Glycerol monostearate (GMS) was selected as crystallizing surface-active lipid, as it has convenient thermal properties for this approach; pure GMS melts at 60–70°C and crystallizes in the temperature range of 57–65°C. Above its melting temperature, GMS can be processed by various emulsification methods, such as mechanical homogenization, pressure-based membrane emulsification, or using microfluidic device technology [3]. GMS is an organic ester

Abbreviations: DC, direct current; GMS, glycerol monostearate; MCT, medium-chain triglyceride; PDMS, poly(dimethyl siloxane); PEB, post-exposure bake; PET, polyethylene terephthalate; PVD, physical vapor deposition; QDR, quick drain rinse.

This is an open access article under the terms of the [Creative Commons Attribution-NonCommercial-NoDerivs](https://creativecommons.org/licenses/by-nc-nd/4.0/) License, which permits use and distribution in any medium, provided the original work is properly cited, the use is non-commercial and no modifications or adaptations are made.

© 2025 The Author(s). *European Journal of Lipid Science and Technology* published by Wiley-VCH GmbH.

of glycerol and stearic acid [4] and thus oil soluble. Known as additive E471, it is considered to be of no particular health concern by the *EFSA Panel on Food Additives and Nutrient Sources added to Food*. GMS is used for the stabilization of margarine, to provide body to baked products, and to add texture to ice cream and whipped cream. It is also applied in edible films, and it is of interest to the pharmaceutical industries [5–7].

Droplet generation in a microfluidic device [8–10] has the advantage of producing emulsions with uniform droplet sizes, which is beneficial in view of understanding the impact of formulation parameters such as the choice and concentration of the crystallizing surface-active lipid, the choice of the oil phase, and the interactions between these two materials on droplet size and stability. However, the thermal transition of the droplet interface from liquid to crystalline involving interfacially adsorbed GMS poses a challenge for a microfluidic droplet generator. Over the relatively small distance of 0.5–1.5 cm, a temperature gradient from $>60^{\circ}\text{C}$ to $<6^{\circ}\text{C}$ has to be established and maintained, such that droplets can be formed within the device above the crystallization temperature of GMS, and a crystalline shell can immediately be formed during travel of the droplet from the flow focusing junction to the collection well. In order to achieve this gradient, we combined an on-chip resistive heating structure with a stage cooler on which the distance between heater and cooling surface can be adjusted. Droplet generation by means of a T-junction [11] or flow focusing [12, 13] is an established means of producing emulsions within a chip device in a well-controlled manner, mostly utilized for oil-in-water and water-in-oil droplet generation for encapsulation in the context of diagnostics [14] and biological cell manipulation [15–17]. Although it is relatively straightforward to place a chip device into an environmental enclosure for bulk temperature control, the establishment of a gradient requires local temperature manipulation. Resistive microheaters [18, 19] and IR-B laser radiation supplied through an optical fiber [20] or microscope objective [21] are established and easily implemented means of generating spots of elevated temperature locally. Local cooling is more challenging [22], and a compromise had to be found that balanced the effort of chip microfabrication and space constraints under an optical research microscope with sufficient performance to reach the desired temperature gradient. Therefore, a microfabricated on-chip heater was combined with a Peltier-type microscope cooling stage, which was designed to reach a temperature well below the melting temperature of the crystalline GMS. An additional element is an off-stage hotplate to pre-heat the oil cargo with GMS additive. A multichannel pressure protocol was developed to drive the droplets from the flow-focusing junction all the way into the collection container.

In the context of Pickering emulsions, microfluidic concepts to decorate droplets with solid materials exist [23], but temperature manipulation on microfluidic devices to affect shell compounds with melting points above room temperature has not been reported yet. Such compounds, including GMS, are particularly important for food applications, because obtaining a solid shell does not require chemical processes or specific interactions, such as charge-based attraction. It was intended to show in this technical study that the microfluidic approach, which is—due to the small structure size—affected by rapid temperature equilibration over short distances of μm -to- mm length, is indeed

capable of generating core-shell particles by a simultaneous heating/cooling process. Proof-of-concept was established with an appropriately designed setup compatible with an inverted research microscope, and droplets were successfully produced, collected, and characterized. The presented method is a reliable source of particles, which are readily available for further material property investigations and optimizations.

2 | Materials and Methods

2.1 | Materials

Medium-chain triglyceride (MCT) oil (C8, 99% pure) was purchased from Ketosource (London, UK). GMS was acquired from BLDpharm (Kaiserslautern, Germany). Nile red technical grade was obtained from Sigma-Aldrich (Solna, Sweden). It was diluted with MCT oil to obtain a 1000 ppm solution and filtered through a 13 mm \times 0.45 μm filter (SupelCo) before use. De-ionized water (Milli-Q, 18.2 M Ω) was used as the continuous phase.

2.2 | Oil-Phase Preparation

10 wt % of GMS and 1 wt % of Nile red-oil mixture were added to 89 wt % of MCT oil. The mixture was heated for 1 h at 100°C while being mixed with a magnetic stirrer. The oil phase was then kept in a liquid state at a temperature above 40°C , which is the on-set crystallization temperature of the mixture, before it entered the chip.

2.3 | Microheater Fabrication

The microheater with 375 μm strip width was fabricated on a glass cover slide substrate [24, 25] by means of a photolithography/physical vapor deposition (PVD) procedure at the cleanroom facility MC2, Chalmers University of Technology, Sweden. The glass plate (75 mm \times 25 mm \times 1 mm) was sonicated in an acetone bath for 5 min, quick drain rinse (QDR)-treated, air-dried, and baked at 130°C for 5 min. After cooling down on a metal plate, hexamethyl disilazane (Stangl, Germany) vapor was applied for 1 min at 100°C to the cleaned surface. Microposit S1813 positive photoresist (Shipley, USA) was deposited onto the entire surface of the cover slide and then spin-coated for 60 s (4500 rpm/acc 2000), according to the manufacturer-recommended process, to get ~ 1.3 μm film thickness, followed by a soft baking step (110°C for 2 min) on a hotplate. Exposure was performed using a laser writer (MLA150, Heidelberg), wavelength 375 nm, dose 230 mJ/cm^2 , and laser defocus level 2. The S1813 was developed in Microposit MF-CD 26 developer (Microresist Technology, Germany) for 1 min, and the cover slip was rinsed in water for 1 min and blow-dried. Subsequently, a plasma ash was performed at 50 W 10 sccm O_2 for 30 s (BatchTop m/95, Plasmatherm) to remove residual resist. Thereafter, 5 nm of titanium followed by 100 nm of aluminum were evaporated onto the cover slip (PVD 225 e-beam evaporator, Lesker) at a base pressure of 5×10^{-7} torr. Lift-off was performed in remover REM 400 (Microresist Technology, Germany) overnight. Finally, the cover slip was washed with isopropyl alcohol (IPA), QDR-treated, blow-dried, and packaged. The electrical resistance of the heater

was determined as $R = 210 \Omega$; at $V = 8 \text{ V}$, the electrical power is $p = 0.31 \text{ W}$.

2.4 | Master Fabrication

The droplet generator chip master was fabricated on a single-side polished 2" silicon wafer by means of soft photolithography [26, 27] combined with a lamination process [28, 29] at the cleanroom facility MC2, Chalmers University of Technology, Sweden. The wafer was sonicated in acetone for 3 min, QDR-treated, and blow-dried. Thereafter, the wafer was placed into buffered oxide etch (BOE) solution (ammonium fluoride/hydrofluoric acid, 7:1) for 5 s to remove the native silicon dioxide layer, QDR-treated, and blow-dried, followed by baking at 130°C for 5 min and cooling down on a metal plate. SUEX dry film photoresist (Microresist Technology, Germany) of 40 μm was selected for the desired channel height. The commercial dry film consisted of three layers: two protective polyethylene terephthalate (PET) coversheets around the dry photoresist film. According to the manufacturer specification, first the glossy PET coversheet was removed from the SUEX dry film. Thereafter, the film was laminated onto the cleaned wafer, using a commercial laminator (PRO SERIES 3600, GBC) at a temperature of 65°C and a sheet transport speed of 5 mm/s. The hazy PET coversheet was removed before the subsequent exposure step. Exposure was performed with a laser writer (MLA150, Heidelberg), at $\lambda = 375 \text{ nm}$, dose 9000–10000 mJ/cm^2 , and laser defocus level 4, appropriate for the low sensitivity negative epoxy resin. Post-exposure bake (PEB) was performed using a benchtop hotplate. The wafer was placed onto the hotplate under a thermoisolating cover and heated from room temperature to 95°C, followed by turning off the hotplate to slowly cool down the wafer for 60 min until reaching room temperature. The dry film was developed in mr-Dev 600 developer for $\sim 5 \text{ min}$, QDR-treated, and blow-dried. Subsequently, the wafer was anti-adhesion-treated with C_7 -perfluoro silane (Sigma-Aldrich) by exposing the surfaces to the vapors in a desiccator for 30 min.

2.5 | Chip Layout

The droplet generator layout [30, 31] was designed in Autodesk AutoCAD 2023 as a conventional flow-focusing junction (cf. Figure S1). Channel dimensions were selected according to the desired droplet size of $\sim 30 \mu\text{m}$. The width of the water supply channel was 100 μm , and 40 μm for the oil/GMS/dye mixture channels. The height of all channels was 40 μm . The orifice width and length at the junction were 40 and 170 μm , respectively.

2.6 | Device Fabrication

The chip device was produced by a soft lithography/replica molding process in poly(dimethyl siloxane) (PDMS) elastomer. PDMS pre-polymer (Sylgard 184, AB Lindberg, Sweden) mixture was divided into two parts; the first aliquot was used to cast the chip body of $\sim 1 \text{ cm}$ height, and the second was spin-coated at 500 rpm/70 s, followed by 2000 rpm/1 min onto the cleaned microheater cover slip to obtain a $\sim 10 \mu\text{m}$ thin PDMS membrane,

which was then cured for 10 min in a convection oven at 95°C. Note: (1) The areas over the heater contact pads, $\sim 9 \text{ mm}^2$ in size, were covered with cleanroom blue tape to prevent coating. (2) It was advisable to not plasma-treat the glass surface before spin deposition, which allowed for the later removal of the PDMS structure and re-use of the heater. The PDMS slab was similarly oven cured, but at 95°C for 45 min. Supply channels were punched into the PDMS body with a $\varnothing 1 \text{ mm}$ biopsy puncher; thereafter, the microheater substrate with PDMS membrane and the PDMS slab were oxygen plasma treated for 1.5 min in an Atto plasma chamber (Diener Electronic, Germany) at 250 mbar, 100 W, and 10 sccm O_2 . Thereafter, the PDMS chip and microheater were manually aligned under a stereomicroscope, using a water film in between the surfaces. The thus assembled chip (cf. Figure S2) was subsequently baked in a convection oven for 10 min at 95°C. Note: If a heated microscope stage is available, the bonding of the aligned chip can be conveniently done without the need to move it. Subsequently, $\varnothing 0.25 \text{ mm}$ silver wire ends of 10 cm length were glued onto the microheater contact pads by acrylic silver glue (Delta Technologies LLC, USA).

2.7 | Microscopy

A Leica DM-IRB2 inverted microscope in a wide-field laser-induced fluorescence setup with 4 \times (numerical aperture [NA] = 0.1) and 10 \times (NA = 0.4) objectives was used for imaging. The Nile red dye tracer [32] was excited at $\lambda_{\text{ex}} = 514 \text{ nm}$ with a diode laser (240 mW, Cobolt 06-MLD, Hubner Photonics, Germany); the emitted light was imaged using a Prosilica GX digital camera (Allied Vision Technologies, Germany).

2.8 | Device Operation

The droplet generator chip was connected via flexible polymer tubing to the pressure source, and its heater was wired to a generic external direct current (DC) power supply with a 1 A current rating before placing it onto the cooling stage (Figure 1). The oil/GMS/dye mixture was too viscous to be pumped directly through the chip. Therefore, the reservoir containing the mixture was placed onto an external hotplate and pre-heated to 60°C. The warm fluid was slowly pumped through the tubing until it reached the outlet and quickly connected to the chip via a hollow needle, such that the enclosed air dead volume was as small as possible. The operation sequence listed in Table 1 was applied to generate the droplets and then collect the particles.

The volumetric flow rate of the droplets was calculated as $Q \sim 2.6 \times 10^{-11} \text{ m}^3/\text{s}$, using the designed channel cross section and motion parameters derived from video recordings (cf. Video S1).

A multichannel pneumatic air pump (Aeolus 500, www.fluidicworks.com) was used to generate the three supply pressures: water and oil/GMS/dye drive pressures p_1 and p_2 , and collection vacuum V (cf. Figure 2). Particles were collected over a time period of 50 min into a 1.5 mL glass vial placed on the cooling plate.

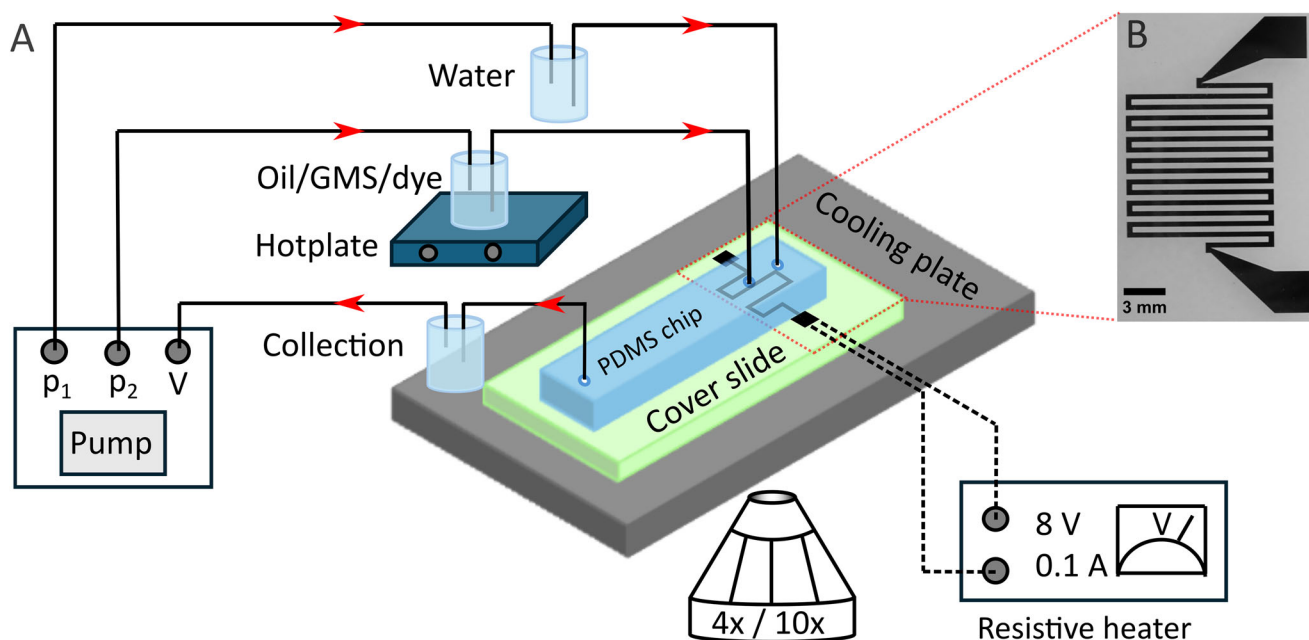


FIGURE 1 | Schematic experimental setup for the generation of GMS crystal-enveloped oil-in-water droplets: (A) arrangement and connectivity of the main components (not to scale); (B) micrograph inset of the resistive microheater structure present on the microfluidic chip substrate surface. GMS, glycerol monostearate; PDMS, poly(dimethyl siloxane).

TABLE 1 | Operation sequence for the heater-cooler setup.

Sequence	Channel on cooling plate	On-chip heater	Droplet generation	Cooling plate	Oil hotplate	Pressure		
						p_1 /mbar (water)	p_2 /mbar (oil)	V /mbar (vacuum)
1 (fill)	NO	OFF	NO	ON	ON	140	100	190
2 (setup)	YES	ON	YES	ON	ON	140	120	190
3 (droplet generation)	YES	ON	YES	ON	ON	140	180	190

2.9 | Droplet Images

A particle suspension of 70 μL drawn from the collection vial was dispensed onto a 24 mm \times 60 mm rectangular #1 cover slide using an automatic micropipette.

2.10 | Image Processing

Images were analyzed with the ImageJ/Fiji software package (National Institutes of Health, USA). Raw micrographs and videos were adjusted for the figures for brightness and contrast.

3 | Results and Discussion

3.1 | Droplet Generator Setup

The challenge of implementing a close-space temperature gradient on a microfluidic chip was met by a combination of on-chip resistive heating and an in-house-made Peltier cooling stage

fitted to an inverted research microscope. The setup provided a temperature gradient from 60°C to 6°C over a distance of \sim 5 mm. The resistive heater was fabricated on a transparent glass slide, which allowed for observation of the channel junction during the droplet generation process and adjustment of the flow rates. Low magnification objectives with a working distance exceeding 1 mm were used for imaging; therefore, the slide thickness was appropriate. #1 cover slips can be used if higher magnification is desired, but due to their fragility, fabrication and handling of the chip are less convenient. Three individual pressure sources were applied, p_1 and p_2 to drive the fluids, and an additional base vacuum V to support the transport of particles into the collection container. Differential pressure sources have been used in earlier microfluidics applications in order to achieve desired flow configurations [33]. Figure 2A shows schematically the layout of the device with the applied pressures. A start-up sequence was established (Table 1), which ensured that the channel does not become clogged by large deposits of semi-solid oil/GMS plugs while establishing droplet formation. To avoid gas bubble generation by overheating the junction, the resistive heater was adjusted to not exceed 80°C, a temperature at which

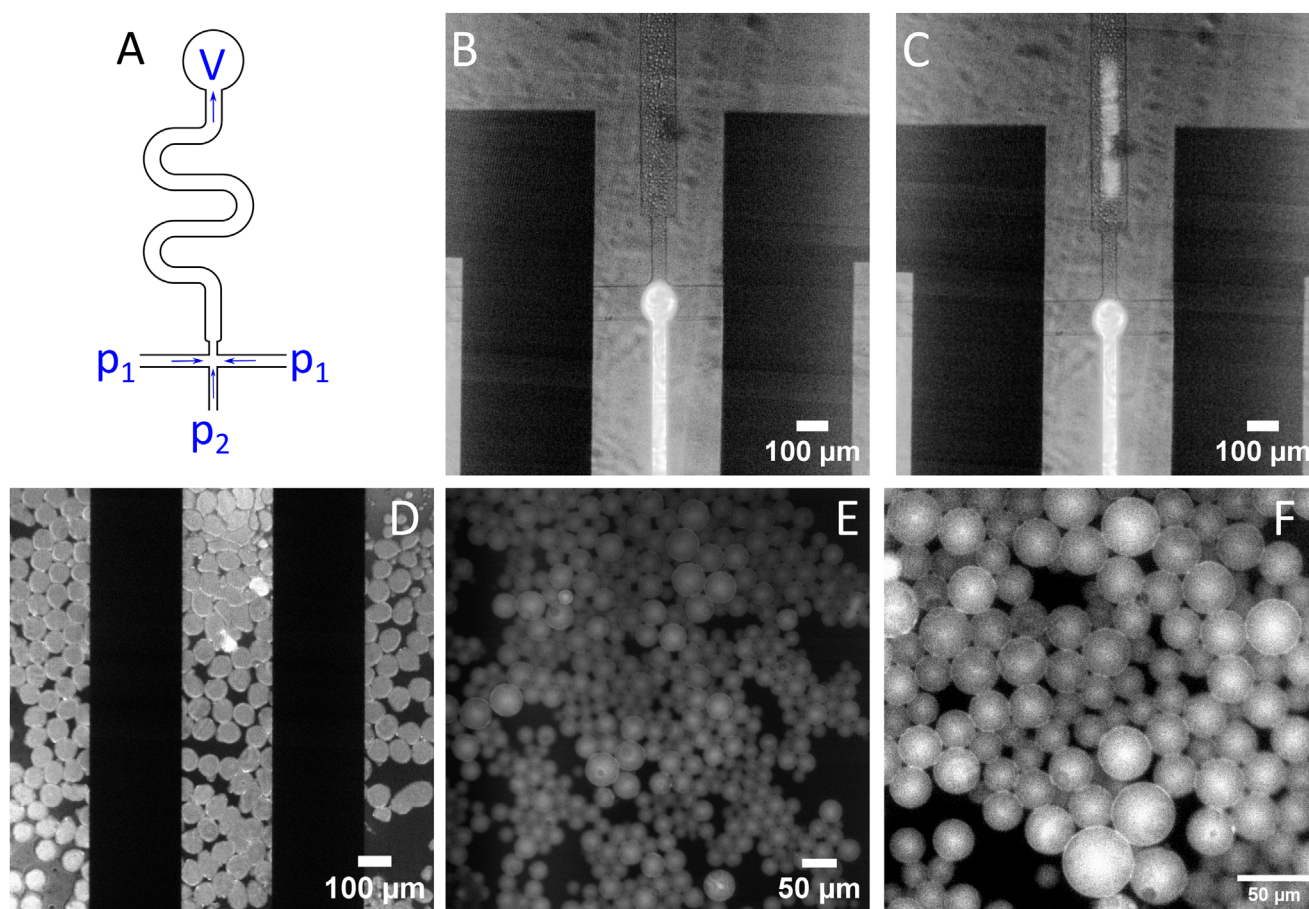


FIGURE 2 | (A) Schematic drawing of the droplet generator chip layout (not to scale). p_1 drives the water phase, p_2 the oil/GMS/dye mixture, and vacuum V increases the overall flow rate for the transport of droplets into the collection container. (B) Brightfield/fluorescence overlay micrograph at 4× magnification of the droplet generation regime at the flow focusing junction. The dark rectangular shadows arise from the surface-printed heating structures, aligned to the channels to keep the junction visible. (C) Micrograph of the same junction during droplet generation. The droplet appears as a plug in the images and is overly elongated due to the low frame rate of the camera. (D) Micrograph of the exit well region at 4× magnification, where the cooling of the droplets was limited to the well region, such that flattened particles were produced. (E and F) Micrographs at 10× magnification of a sample after collection, formed when cooling the entire length of the formation channel. The images were taken 50 min after commencing droplet formation. Note that the surface-printed structures over the collection well are only half as wide as those over the junction.

the oil mixture was just sufficiently fluid to be processed in the chip. Before generating droplets on the microscope stage, the chip was placed on the external hotplate, and Step 1 of the start-up procedure was performed, such that oil filled the dead volume and reached the junction. Note that this step can alternatively be performed on-stage by using a second heater placed across the outlet well of the chip (cf. Figure S2). Thereafter, the chip was immediately placed on the cooling stage such that the distance between heating and cooling regions was >1.5 cm, followed by increasing the flow rate of the oil mixture (Step 2 in Table 1). Once the droplet formation had stabilized, the chip was translocated such that the distance between heating and cooling regions was reduced to ~5 mm, followed by increasing the pressure of oil/GMS/dye mixture (Step 3 in Table 1). Figure 2B,C displays brightfield/fluorescence overlay micrographs showing the flow focusing junction with the oil mixture enveloped by the perpendicular water streams (B) and the shearing off of a droplet. Due to the limited frame rate of the camera, the droplet appears as an overly elongated plug in (C). Figure 2D is a micrograph of the particles that formed when the chip was not properly primed according to the start-up sequence. Although the particles were

of good size homogeneity, they appeared flattened and adhered to the surface of the collection well. This resulted when the transition from fluid droplets to particles occurred in the region of the collection well rather than in the channel connecting the channel junction. When the channel was appropriately placed over the cooling surface of the stage in Step 3 of the sequence, individual spherical particles formed consistently and could be collected (Figure 2E,F).

3.2 | Particle Size Characterization

Aliquots of the particle suspension, collected in a 1.5 mL glass vial (Sample 1, cf. Video S2) and rested in a refrigerator (4°C) for 5 days (Sample 2, cf. Video S3), were subjected to size analysis (Figure 3, cf. Figure S3). The center fraction of Sample 1 consisted of 31 μm spherical particles; the population was unevenly distributed over a range from 13 to 49 μm. In a second sample, analyzed after a period of 5 days, the fractions of larger particles had decreased in number. After resting, the particles in this sample were considerably less clustered, and the observed

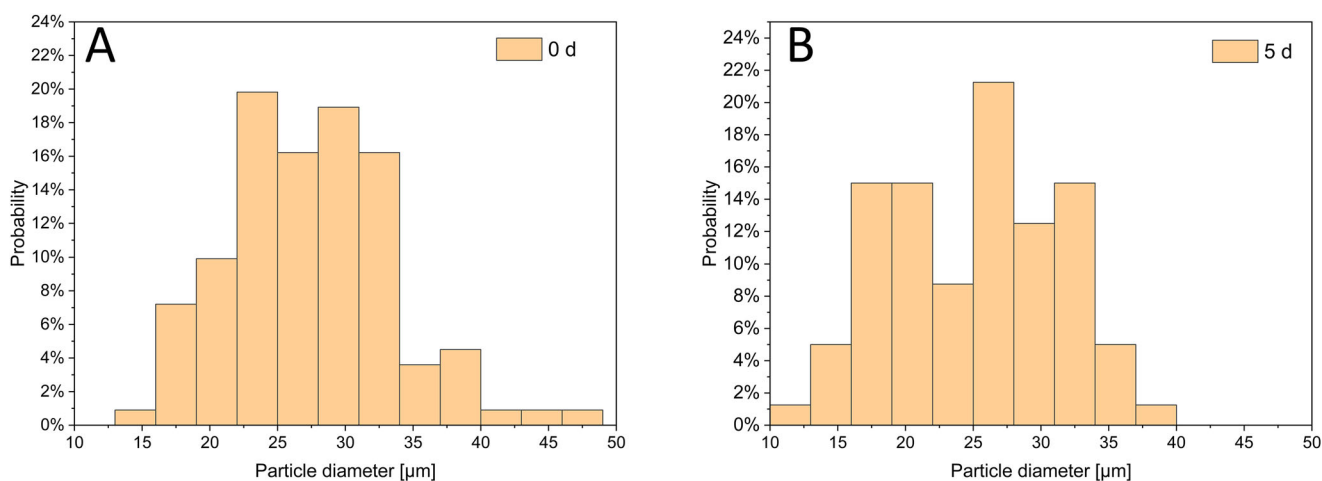


FIGURE 3 | (A) Particle size distribution bar graph for Sample 1. The total number of particles is 111. (B) Bar graph for Sample 2 consisting of 80 particles. Both samples were generated at $p_1 = 140$ mbar, $p_2 = 180$ mbar, and $V = 190$ mbar. Sample 1 was analyzed immediately after collection, and Sample 2 after 5 days of resting time.

decrease was related to sampling; that is, the small amount ($\sim 3\%$ in Sample 1) of very large particles was not represented in Sample 2. Independent from the time of analysis, the size distribution was comparatively wide compared to the visibly narrower distribution of the flattened particles seen in Figure 2D. Size distribution in a T-junction device has recently been investigated carefully, using an oil/water system. Distributions with a coefficient of variation between 5.5% and 11% were determined [34], which represents particle output much narrower in size distribution than what we achieved.

In our system, a fraction of particles smaller than expected for the channel size was present. We do not attribute this discrepancy to random merging of particles of smaller size after generation but rather to undesired instabilities in the droplet generation regime. This is very likely linked to the short temperature gradient, given the more homogeneous particle size around a value expected from the device design when the temperature gradient is established over a distance larger by an order of magnitude (cf. Figure 2D) [35]. One possible explanation is the limited accuracy of the temperature setting at the channel junction. The resistive heater is operated in a constant voltage mode; it is not controlled through a feedback loop [18] and therefore prone to fluctuations, particularly when confronted with a nearby active heat sink. This possibly leads to viscosity and interfacial tension variations in the fluids, which are quite significant in magnitude even for small temperature fluctuations [36]. More elaborate image recording with a high frame rate camera could be utilized to investigate this further, and a feedback loop would be of advantage, requiring only an additional surface-printed temperature sensor to be placed within the heater structure [37].

4 | Conclusions

The study at hand represents proof of concept of a microfluidic droplet generator implementing closed-space heating-cooling to establish a short-distance temperature gradient, spanning $\sim 60^\circ\text{C}$ over 5 mm. Selecting GMS as the oil-soluble surface-

active crystallizing lipid, it was demonstrated that this device is capable of producing an aqueous suspension of lipid-crystallized shell liquid-core particles from oil-in-water droplets containing the crystallizing stabilizer in the oil phase. The setup is moderate in its requirements: A resistive heater was micro-fabricated on the chip substrate, replica molding was utilized for chip generation, and off-the-shelf instrumentation was used to supply the device. An operation procedure was developed that allows for continuous production and collection of droplets. The device is, due to the volume flow limitation of microfluidic devices, not directly scalable for large-scale production, but has potential for parallelization. We have shown that the length of the temperature gradient is essential for consistent droplet generation over long periods of time. The determined size distribution of the collected particles is relatively wide in comparison to conventional constant temperature droplet generators, an issue likely linked to temperature instabilities, which will be subject to further analysis and optimization.

Author Contributions

Rui Liu performed fabrication, droplet generation, and microscopy experiments and analyzed data. Aldo Jesorka designed the experiments, assembled the cooling stage, performed data analyses and evaluation, and supervised the project. Carolina Gomez Guarguati designed the material system and contributed material property data. Aldo Jesorka, Eddie Pelan, and Bettina Wolf acquired the funding. All authors contributed substantially to the writing of the manuscript.

Acknowledgments

We thank the engineers of the Microtechnology Center MC2 for their support. The authors acknowledge funding by the European Union's Horizon 2020 research and innovation program under the Marie Skłodowska-Curie grant agreement no. 956248.

Conflicts of Interest

Aldo Jesorka is the developer of the Aeolus 500 multichannel pump.

Data Availability Statement

The data that were generated during the current study are available from the corresponding author on reasonable request.

References

- X. L. Zhang, Q. L. Qu, A. Zhou, et al., "Core-Shell Microparticles: From Rational Engineering to Diverse Applications," *Advances in Colloid and Interface Science* 299 (2022): 102568.
- M. Douaire, V. Di Bari, J. E. Norton, A. Sullo, P. Lillford, and I. T. Norton, "Fat Crystallisation at Oil-Water Interfaces," *Advances in Colloid and Interface Science* 203 (2014): 1–10.
- L. J. Chen, F. Ao, X. M. Ge, and W. Shen, "Food-Grade Pickering Emulsions: Preparation, Stabilization and Applications," *Molecules (Basel, Switzerland)* 25 (2020): 3202.
- K. Sharma, S. Negi, N. Thakur, and K. Kishore, "Partial Glycerides-An Important Nonionic Surfactant for Industrial Applications: An Overview," *Journal of Biological and Chemical Chronicles* 3 (2017): 10–19.
- F. R. Lupi, V. Mancina, N. Baldino, O. I. Parisi, L. Scrivano, and D. Gabriele, "Effect of the Monostearate/Monopalmitate Ratio on the Oral Release of Active Agents From Monoacylglycerol Organogels," *Food & Function* 9 (2018): 3278–3290.
- J. B. Lauridsen, "Food Emulsifiers—Surface-Activity, Edibility, Manufacture, Composition, and Application," *Journal of the American Oil Chemists Society* 53 (1976): 400–407.
- EFSA Panel on Food Additives and Nutrient Sources Added to Food (ANS). M. Younes, P. Aggett, et al., "Re-Evaluation of Mono- and Di-Glycerides of Fatty Acids (E 471) as Food Additives," *EFSA Journal* 15 (2017): 05045.
- E. Piccin, D. Ferraro, P. Sartori, E. Chiarello, M. Pierno, and G. Mistura, "Generation of Water-in-Oil and Oil-in-Water Microdroplets in Polyester-Toner Microfluidic Devices," *Sensors and Actuators B-Chemical* 196 (2014): 525–531.
- S. Sahin and K. Schroën, "Partitioned EDGE Devices for High Throughput Production of Monodisperse Emulsion Droplets With Two Distinct Sizes," *Lab on a Chip* 15 (2015): 2486–2495.
- M. Seo, C. Paquet, Z. H. Nie, S. Q. Xu, and E. Kumacheva, "Microfluidic Consecutive Flow-Focusing Droplet Generators," *Soft Matter* 3 (2007): 986–992.
- P. Garstecki, M. J. Fuerstman, H. A. Stone, and G. M. Whitesides, "Formation of Droplets and Bubbles in a Microfluidic T-Junction—Scaling and Mechanism of Break-Up," *Lab on a Chip* 6 (2006): 437–446.
- P. Dunkel, Z. Hayat, A. Barosi, et al., "Photolysis-Driven Merging of Microdroplets in Microfluidic Chambers," *Lab on a Chip* 16 (2016): 1484–1491.
- P. K. Shivhare, A. Prabhakar, and A. K. Sen, "Optofluidics Based Lab-on-Chip Device for Measurement of Mean Droplet Size and Droplet Size Distribution of an Emulsion," *Journal of Micromechanics and Microengineering* 27 (2017): 035003.
- A. M. Nightingale, C. L. Leong, R. A. Burnish, et al., "Monitoring Biomolecule Concentrations in Tissue Using a Wearable Droplet Microfluidic-Based Sensor," *Nature Communications* 10 (2019): 2741.
- P. K. P. Rajeswari, H. N. Joensson, and H. Andersson-Svahn, "Droplet Size Influences Division of Mammalian Cell Factories in Droplet Microfluidic Cultivation," *Electrophoresis* 38 (2017): 305–310.
- N. Shembekar, H. X. Hu, D. Eustace, and C. A. Merten, "Single-Cell Droplet Microfluidic Screening for Antibodies Specifically Binding to Target Cells," *Cell Reports* 22 (2018): 2206–2215.
- N. Wen, Z. Zhao, B. Y. Fan, et al., "Development of Droplet Microfluidics Enabling High-Throughput Single-Cell Analysis," *Molecules (Basel, Switzerland)* 21 (2016): 881.
- H. Bridle, M. Millingen, and A. Jesorka, "On-Chip Fabrication to Add Temperature Control to a Microfluidic Solution Exchange System," *Lab on a Chip* 8 (2008): 480–483.
- M. Markström, A. Gunnarsson, O. Orwar, and A. Jesorka, "Dynamic Microcompartmentalization of Giant Unilamellar Vesicles by Sol–Gel Transition and Temperature Induced Shrinking/Swelling of Poly (N-Isopropyl Acrylamide)," *Soft Matter* 3 (2007): 587–595.
- K. Spustova, L. Xue, R. Ryskulov, A. Jesorka, and I. Gozen, "Manipulation of Lipid Membranes With Thermal Stimuli," *Methods in Molecular Biology* 2402 (2022): 209–225.
- R. Ryskulov, E. Pedrueza-Villalmanzo, Y. A. Tatli, I. Gozen, and A. Jesorka, "Complete De-Wetting of Lipid Membranes on Silicon Carbide," *European Physical Journal-Special Topics* 233 (2024): 2743–2756.
- D. F. Sun, X. Han, H. Q. Wang, et al., "Investigation on the Linear Cooling Method of Microfluidic Chip Based on Thermoelectric Cooler," *Energy* 308 (2024): 132933.
- A. Schröder, J. Sprakel, K. Schroën, J. N. Spaen, and C. C. Berton-Carabin, "Coalescence Stability of Pickering Emulsions Produced With Lipid Particles: A Microfluidic Study," *Journal of Food Engineering* 234 (2018): 63–72.
- J. P. Hilton, T. Nguyen, M. Barbu, R. J. Pei, M. Stojanovic, and Q. Lin, "Bead-Based Polymerase Chain Reaction on a Microchip," *Microfluidics and Nanofluidics* 13 (2012): 749–760.
- R. Phatthanakun, P. Deekla, W. Pummara, C. Sriphung, C. Pantong, and N. Chomnawang, "Design and Fabrication of Thin-Film Aluminum Microheater and Nickel Temperature Sensor," in *IEEE International Conference on Nano/Micro Engineered and Molecular Systems*, (IEEE, 2012), 112–115.
- D. Qin, Y. N. Xia, and G. M. Whitesides, "Soft Lithography for Micro- and Nanoscale Patterning," *Nature Protocols* 5 (2010): 491–502.
- Y. N. Xia and G. M. Whitesides, "Soft Lithography," *Angewandte Chemie-International Edition* 37 (1998): 550–575.
- N. E. Koucherian, S. J. Yan, and E. E. Hui, "Fabrication of Multilayer Molds by Dry Film Photoresist," *Micromachines* 13 (2022): 1583.
- P. Mukherjee, F. Nebuloni, H. Gao, J. Zhou, and I. Papautsky, "Rapid Prototyping of Soft Lithography Masters for Microfluidic Devices Using Dry Film Photoresist in a Non-Cleanroom Setting," *Micromachines* 10 (2019): 192.
- Y. C. Tan, J. S. Fisher, A. I. Lee, V. Cristini, and A. P. Lee, "Design of Microfluidic Channel Geometries for the Control of Droplet Volume, Chemical Concentration, and Sorting," *Lab on a Chip* 4 (2004): 292–298.
- A. Y. Tenorio-Barajas, M. de la Luz Olvera-Amador, V. Altuzar, R. Ruiz-Ramos, M. A. Palomino-Ovando, and C. Mendoza-Barrera, "Microdroplet Formation in Microfluidic Channels by Multiphase Flow Simulation," in *16th International Conference on Electrical Engineering, Computing Science and Automatic Control (CCE)*, (IEEE, 2019), 1–5.
- P. Raudsepp, D. A. Brüggemann, and M. L. Andersen, "Detection of Radicals in Single Droplets of Oil-in-Water Emulsions With the Lipophilic Fluorescent Probe BODIPY and Confocal Laser Scanning Microscopy," *Free Radical Biology and Medicine* 70 (2014): 233–240.
- A. Ainla, G. D. M. Jeffries, R. Brune, O. Orwar, and A. Jesorka, "A Multifunctional Pipette," *Lab on a Chip* 12 (2012): 1255–1261.
- J. U. Alvarez-Martínez, O. Medina-Cázares, A. González-Vega, G. Segura-Gómez, G. Gutiérrez-Juárez, and R. Castro-Beltrán, "Microfluidic Droplet Generation: An Experimental Study of Size Distribution Using Probability Density Function Analysis," *Journal of Micromechanics and Microengineering* 35 (2025): 015001.
- P. Laval, J. B. Salmon, and M. Joanicot, "A Microfluidic Device for Investigating Crystal Nucleation Kinetics," *Journal of Crystal Growth* 303 (2007): 622–628.
- N.-T. Nguyen, T.-H. Ting, Y.-F. Yap, et al., "Thermally Mediated Droplet Formation in Microchannels," *Applied Physics Letters* 91 (2007): 084102.

37. F. Le Goupil, G. Payrot, S. Khiev, W. Smaal, and G. Hadziioannou, "Fully Printed Sensors for In Situ Temperature, Heat Flow, and Thermal Conductivity Measurements in Flexible Devices," *ACS Omega* 8 (2023): 8481–8487.

Supporting Information

Additional supporting information can be found online in the Supporting Information section.

Supporting File 1: ejlt70066-sup-0001-SuppMat.docx.

Supporting Video 1: ejlt70066-sup-0002-Video1.avi.

Supporting Video 2: ejlt70066-sup-0003-Video2.avi.

Supporting Video 3: ejlt70066-sup-0004-Video3.avi.